

OPEN

Rectal Cancer Invasiveness: Whole-Lesion Diffusion-Weighted Imaging (DWI) Histogram Analysis by Comparison of Reduced Field-of-View and Conventional DWI Techniques

Yang Peng¹, Hao Tang¹, Xuemei Hu¹, Yaqi Shen¹ , Ihab Kamel², Zhen Li^{1*} & Daoyu Hu¹

To explore the role of whole-lesion histogram analysis of apparent diffusion coefficient (ADC) for discriminating between T stages of rectal carcinoma by comparison of reduced field-of-view (FOV) and conventional DWI techniques. 102 patients with rectal cancer were enrolled in this retrospective study. All patients received preoperative MR scan at 3T, including reduced and full FOV DWI sequences. Histogram parameters from two DWI methods were calculated and correlated with histological T stage of rectal cancer. The diagnostic performance of individual parameter for differentiating stage pT1-2 and pT3-4 tumors from both DWI techniques was assessed by receiver operating characteristic curve analysis. There were significant differences for the parameters of ADCmean, 50th, 75th, 90th, 95th percentiles, skewness and kurtosis of both DWI sequences in patients with pT1-2 as compared to those with pT3-4 tumors ($P < 0.05$), in addition to parameters including ADCmin ($P = 0.015$) and 25th percentile ($P = 0.006$) from rFOV DWI. Correlations were noted between T staging and above histogram parameters from rFOV DWI ($r: -0.741-0.682$) and fFOV DWI ($r: -0.449-0.449$), besides parameters of ADCmin (0.370) and 25th percentile (-0.425) from rFOV DWI. The AUCs of 75th and 90th percentiles from rFOV DWI were significantly higher than that from fFOV DWI ($P = 0.0410$ and $P = 0.0208$). The whole-lesion histogram analysis based on rFOV DWI was overall more advantageous than the one based on fFOV DWI in differentiating T staging of rectal cancer and the 90th percentile ADC from rFOV DWI was the value with the highest AUC (0.932).

Colorectal cancer is one of the most common cancers ranking the third in men and the second in women all over the world¹ and is reported to have a locally recurrent rate of 3% to 20.6% after surgical resection^{2,3}. The prognosis of rectal cancer is highly dependent on the early detection and accurate staging⁴. The utility of total mesorectal excision (TME) surgery and followed neoadjuvant chemoradiotherapy has been the priority treatment for locally advanced rectal carcinoma (those with tumor invasion into perimesorectal fat and/or involvement of pelvic or mesorectal lymph nodes (cT3-4N0M0 or any T0N1M0)) with remarkable reduction of local recurrence rates^{5,6}. However, excessive or insufficient treatment would lead to possible genitourinary function impairment and local recurrence^{7,8}. Accurate T staging is essential to identify proper patients who are most likely to benefit from above combination treatment⁹.

MR imaging has been widely accepted as the optimum imaging modality for staging of rectal cancer and guiding treatment¹⁰⁻¹³. However, given to the utility of lower resolution MR techniques and thicker sections, discrimination of tumor invasion within muscular layer of rectum from tumor invasion by penetration through

¹Department of Radiology, Tongji Hospital, Tongji Medical College, Huazhong University of Science and Technology, 1095 Jiefang Avenue, Wuhan, Hubei, 430030, P.R. China. ²Russell H. Morgan Department of Radiology and Radiological Science, The Johns Hopkins Medical Institutions, Baltimore, Maryland, 21287, USA. *email: zhenli@hust.edu.cn

Variable	NO. Patient (%)
Age (years)	56.2 ± 12.2 (22–82) ^a
Gender	
Male	34 (69.4)
Female	15 (30.6)
Distance of primary mass from anal verge	
0–5.0 cm	23 (46.9)
5.1–10.0 cm	18 (36.7)
10.1–15.0 cm	8 (16.3)
TNM stage	
T category	
T1	2 (4.1)
T2	19 (38.8)
T3	20 (40.8)
T4	8 (16.3)
N category	
N0	31 (63.3)
N1/2	18 (36.7)
M category	
M0	43 (87.8)
M1	6 (12.2)
Histological differentiation	
Well	10 (20.4)
Moderately	15 (30.6)
Poorly	24 (49.0)
Tumor volume	10.28 ± 6.84 (0.94–31.38) ^a

Table 1. Patient and tumor characteristics. ^aMean ± SD (range); Tumor volume is given in units of cm³.

muscular layer even the whole rectal wall is sometimes challenging. More importantly, it is difficult to distinguish desmoplastic and inflammatory reactions from real tumor status because they all have similar invading behaviors of penetration through muscular rectal walls¹⁴. Therefore, improved MR techniques are needed for clinical management.

DWI is a noninvasive functional imaging tool for characterization of tumors, prognosis and response evaluation of different malignant cancers^{11,15,16}. The ADC obtained from regions of interest (ROI) in DWI could provide quantitative information for cancerous tissues. As for rectal cancers, it has been reported that the ADC values were statistically significant between different T stages of tumors and ADC values could become an imaging biomarker reflecting tumor aggressiveness^{17–19}. Moreover, the conventional DWI (fFOV DWI) technique, based on single-shot echo-planar imaging, can easily bring about distortions and artifacts²⁰ because of its vulnerability to off-resonance due to narrow band width in the phase encoding direction. The reduced field-of-view (rFOV) DWI could provide DWI images with higher image quality and less artifacts, by employment of two-dimensional (2D) spatially-selective echo-planar radiofrequency (RF) pulse, followed by a 180° refocus pulse^{21–24}. This technique could render the lesion margins and internal features of rectal cancer more conspicuously²⁵.

While many studies reported mean ADC values from single slice-based ROIs, whole-lesion histogram analysis of ADC maps has been increasingly recognized for quantitative evaluation of intratumoral heterogeneity and tissue characteristics. One intrinsic feature of tumors is characterized by heterogeneity, which makes tumor tissue distinguished from normal tissue²⁶. The whole-lesion method may better capture heterogeneous tumor areas with various diffusion characteristics demonstrated in the histogram and potential selective sampling bias could be decreased by measurement of whole tumor volumes²⁷. The assessment of tumor heterogeneity has been reported to be highly promising for cancer diagnosis and treatment monitoring^{28–30}. For instance, the ADC histogram analysis has been used for assessing aggressiveness of prostatic cancer³¹, or bladder cancer³² and discriminating adrenal adenoma from pheochromocytoma³³. To date, the utility of whole-lesion histogram analysis based on rFOV DWI for preoperative T staging of rectal cancer has not been reported.

The purpose of this study was to explore the role of whole-lesion histogram analysis in assessment of histological T staging of rectal cancer by comparison of fFOV DWI and rFOV DWI techniques.

Results

Baseline characteristics. The baseline characteristics for patients and lesions of rectal cancers are shown in Table 1. All the 49 patients underwent surgery, and the histopathological results revealed 2 (4.1%) T1 stage, 19 (38.8%) T2 stage, 20 (40.8%) T3 stage and 8 (16.3%) T4 stage. There was significant difference between male age and female age (52.76 ± 11.27 vs. 64.00 ± 10.70, $P = 0.002$). Significant differences between male and female groups occurred in many histogram parameters based on rFOV DWI and conventional DWI, and the values of histogram parameters of female group were significantly higher than those of male group ($P < 0.05$) for both

Parameter /DWI technique	T1-2 (N = 21)	T3-4 (N = 28)	P-value	Correlation coefficient (T staging)	P-value
ADCmean					
rFOV DWI	1198.55 ± 138.55	1057.30 ± 59.76	<0.001	-0.601 (-0.783, -0.373)	<0.001
fFOV DWI	1163.26 ± 144.97	1076.50 ± 82.67	0.011	-0.309 (-0.549, -0.027)	0.031
ADCmin					
rFOV DWI	188.33 ± 169.46	313.57 ± 173.79	0.015	0.370 (0.106, 0.608)	0.009
fFOV DWI	423.57 ± 264.64	546.25 ± 277.76	0.125	0.155 (-0.127, 0.403)	0.289
25th percentile ADC					
rFOV DWI	956.73 ± 122.48	882.37 ± 55.72	0.006	-0.425 (-0.662, -0.132)	0.002
fFOV DWI	963.04 ± 141.83	907.32 ± 74.54	0.081	-0.223 (-0.504, 0.093)	0.123
50th percentile ADC					
rFOV DWI	1154.88 ± 150.04	1017.95 ± 58.61	0.001	-0.582 (-0.770, -0.334)	<0.001
fFOV DWI	1122.62 ± 153.13	1028.84 ± 83.06	0.008	-0.356 (-0.575, -0.105)	0.012
75th percentile ADC					
rFOV DWI	1408.10 ± 158.13	1184.69 ± 72.15	<0.001	-0.726 (-0.825, -0.568)	<0.001
fFOV DWI	1329.35 ± 155.40	1196.34 ± 100.23	0.001	-0.449 (-0.654, -0.190)	0.001
90th percentile ADC					
rFOV DWI	1653.76 ± 191.15	1388.86 ± 93.16	<0.001	-0.741 (-0.837, -0.573)	<0.001
fFOV DWI	1545.81 ± 176.32	1396.41 ± 126.94	0.001	-0.424 (-0.633, -0.152)	0.002
95th percentile ADC					
rFOV DWI	1807.04 ± 227.21	1550.63 ± 122.67	<0.001	-0.647 (-0.787, -0.454)	<0.001
fFOV DWI	1689.75 ± 212.16	1543.65 ± 172.10	0.011	-0.362 (-0.604, -0.091)	0.011
Skewness					
rFOV DWI	0.65 ± 0.40	1.18 ± 0.43	<0.001	0.560 (0.321, 0.734)	<0.001
fFOV DWI	0.70 ± 0.60	1.25 ± 0.48	0.001	0.423 (0.151, 0.653)	0.002
Kurtosis					
rFOV DWI	0.88 ± 0.94	3.26 ± 2.04	<0.001	0.682 (0.514, 0.806)	<0.001
fFOV DWI	1.28 ± 1.21	3.01 ± 2.15	0.001	0.499 (0.243, 0.688)	<0.001

Table 2. Comparison of whole-lesion histogram parameters between T1-2 and T3-4 stages of rectal cancer based on rFOV DWI and fFOV DWI techniques. Note. — data are means and standard deviations (averages between readers). ADC values are given in units of 10^{-6} mm²/s. Data in parentheses are 95% confidence intervals.

DWI techniques. But there was no significant difference between rFOV DWI and conventional DWI for the diagnostic efficacy of the same histogram parameter in relation to gender ($P > 0.05$). The tumor volume ranged from 0.94 cm³ to 31.38 cm³, and the mean tumor volume was 10.28 ± 6.84 cm³.

Interobserver and intraobserver variability. The histogram parameters of rFOV DWI technique had excellent interobserver and intraobserver agreement ($P < 0.001$ for each parameter). The histogram parameters of fFOV DWI technique showed good to excellent interobserver and intraobserver agreement ($P < 0.001$ for each parameter). As for the interobserver agreement, the ICC values ranged from 0.954 to 0.993 for rFOV DWI, and the ICC values ranged from 0.700 to 0.992 for fFOV DWI. As for intraobserver agreement, the ICC values ranged from 0.967 to 0.996 for rFOV DWI, and the ICC values ranged from 0.783 to 0.990 for fFOV DWI.

Comparison of histogram parameters between T1-2 and T3-4 stages of rectal cancer based on rFOV DWI and fFOV DWI techniques. As for rFOV DWI, there was significant difference found in ADCmean, 75th percentile ADC, 90th percentile ADC, 95th percentile ADC, skewness, kurtosis ($P < 0.001$ for all), ADCmin ($P = 0.015$), 25th percentile ADC ($P = 0.006$) and 50th percentile ADC ($P = 0.001$). As for fFOV DWI, significant difference was found in 75th percentile ADC, 90th percentile ADC, skewness, kurtosis ($P = 0.001$ for all), ADCmean, 95th percentile ADC ($P = 0.011$ for both), and 50th percentile ADC ($P = 0.008$) (Table 2). The difference of other parameters such as ADCmax, 5th, 10th percentiles, tumor volume and entropy was not significant for both DWI techniques.

With respect to the parameters from rFOV DWI, there were significant correlations between T staging and following parameters (Table 2): ADCmean, 50th percentile ADC, 75th percentile ADC, 90th percentile ADC, 95th percentile ADC, skewness, kurtosis ($P < 0.001$), ADCmin ($P = 0.009$), and 25th percentile ADC ($P = 0.002$). Among the parameters, 90th percentile ADC demonstrated the strongest correlation of -0.741 with T staging (95% CI: $-0.837, -0.573$), while kurtosis showed the highest correlation of 0.682 with T staging (95% CI: $0.514, 0.806$). There was also a positive correlation found between ADCmin and T staging (0.370 ; 95% CI: $0.106, 0.608$). As for the parameters from fFOV DWI, significant correlations were observed between T staging and following parameters: ADCmean ($P = 0.031$), 50th percentile ADC ($P = 0.012$), 75th percentile ADC ($P = 0.001$), 90th percentile ADC ($P = 0.002$), 95th percentile ADC ($P = 0.011$), skewness ($P = 0.002$), and kurtosis ($P < 0.001$). 75th

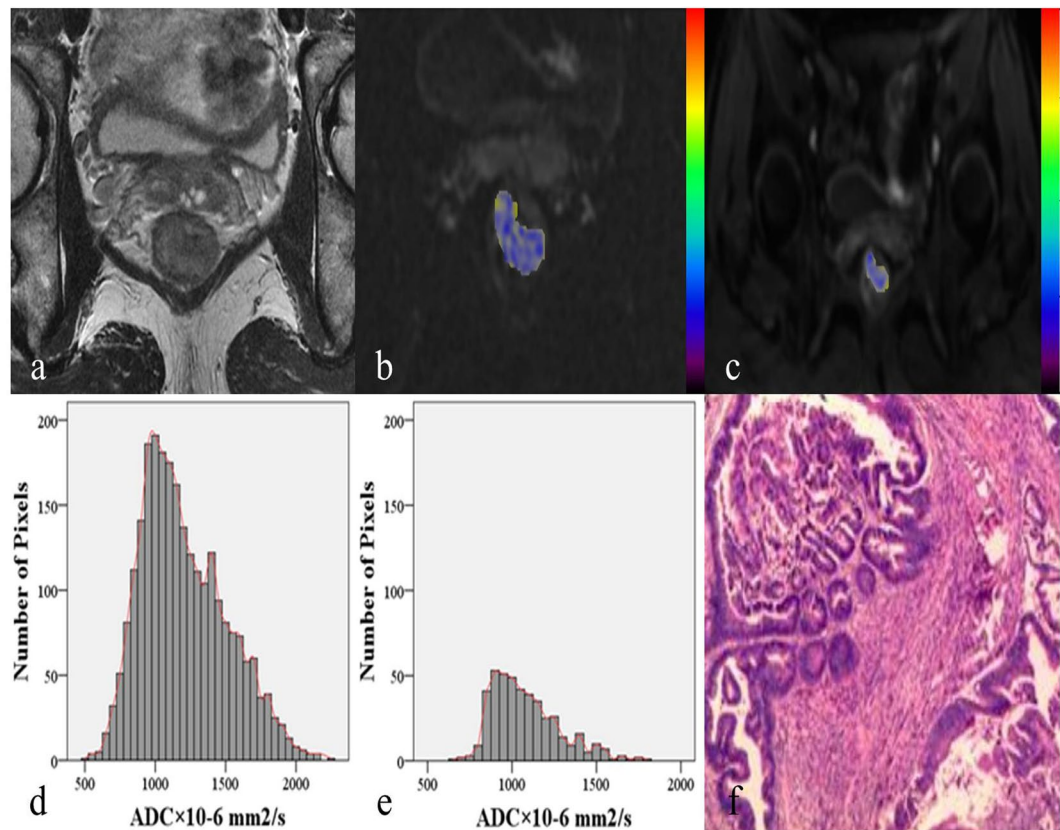


Figure 1. A 46-year-old female patient with T2 stage rectal adenocarcinoma. (a) Axial T2-weighted image showing intra-luminal lesion with intermediate signal intensity in the lower segment of rectum. (b,c) Corresponding diffusion-weighted images of rFOV DWI and fFOV DWI with the identical lesion for reconstruction of ADC measurements. (d,e) Whole-lesion histograms of rFOV DWI and fFOV DWI. F: Histopathological H&E (hematoxylin & eosin staining, $\times 100$) image shows a moderately-differentiated adenocarcinoma invading the muscular layer of rectal wall.

percentile ADC had the relatively strongest correlation of -0.449 with T staging (95% CI: $-0.654, -0.190$), while kurtosis showed the highest correlation of 0.449 with T staging (95% CI: $0.243, 0.688$). Representative cases from two DWI techniques to demonstrate different T staging of rectal cancer are shown in Figs. 1 and 2 respectively.

Comparison of ROC analysis of parameters for T1-2 vs. T3-4 stage tumors based on rFOV DWI and fFOV DWI techniques.

According to the ROC analysis test from rFOV DWI, the 90th percentile ADC demonstrated the highest AUC of 0.932 (95% CI: $0.860, 1.000$) in distinguishing pT1-2 and pT3-4 stages of rectal cancer, whereas ADC_{min} achieved the the lowest AUC of 0.714 (95% CI: $0.565, 0.863$). The optimal cutoff value of the 90th percentile ADC was $1527.50 \times 10^{-6} \text{ mm}^2/\text{s}$ with sensitivity of 81.00% and specificity of 92.90% . As for fFOV DWI, kurtosis achieved the highest AUC of 0.791 (95% CI: $0.663, 0.919$) in distinguishing pT1-2 and pT3-4 stages of rectal cancer. However, ADC_{mean} had the lowest AUC of 0.680 (95% CI: $0.527, 0.834$). The optimal cutoff value of kurtosis was 0.984 with sensitivity of 96.40% and specificity of 52.40% (Table 3, Fig. 3). The AUCs of 75th percentile ADC (0.923 vs. 0.762 , $P = 0.0410$) and 90th percentile ADC (0.932 vs. 0.747 , $P = 0.0208$) from rFOV DWI were significantly higher than that from fFOV DWI.

Discussion

In our study, we investigated the role of rFOV DWI and fFOV DWI techniques in assessment of pathological T staging of rectal cancer by using whole-lesion histogram analysis. The results demonstrated that the histogram parameters from both DWI techniques could be utilized to discriminate between pT1-2 and pT3-4 stages of rectal cancer including ADC_{mean}, 50th, 75th, and 95th percentile ADCs, skewness and kurtosis, besides the parameters of ADC_{min} and 25th percentile ADC from rFOV DWI. The AUCs of 75th and 90th percentile ADCs from rFOV DWI were significantly higher than that from fFOV DWI ($P = 0.0410$ and $P = 0.0208$ respectively). The 90th percentile ADC from rFOV DWI achieved the highest AUC (0.932) in differentiating T staging of rectal cancer, with the optimal cutoff value of $1527.50 \times 10^{-6} \text{ mm}^2/\text{s}$. The whole-lesion histogram analysis based on rFOV DWI was more advantageous over that based on fFOV DWI in evaluation of rectal cancer invasiveness.

We also assessed the interobserver and intraobserver variability for whole-lesion histogram parameters from both two DWI techniques. The results showed overall good to excellent agreement. The excellent interobserver

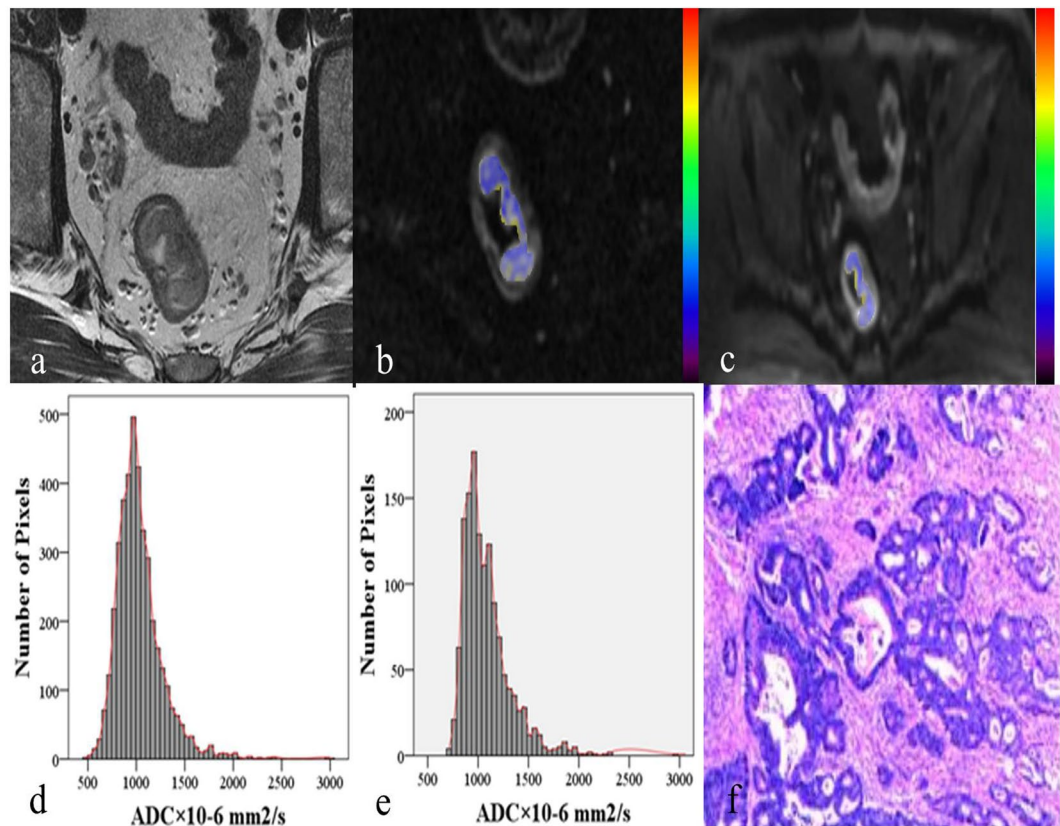


Figure 2. A 42-year-old male patient with T3 stage rectal adenocarcinoma. (a) Axial T2-weighted image showing irregular thickening of rectal wall with intra-luminal mass in the upper segment of rectum. (b,c) Corresponding diffusion-weighted images of rFOV DWI and fFOV DWI with the same lesion for reconstruction of ADC measurements. (d,e) Whole-lesion histograms of rFOV DWI and fFOV DWI. (f) Histopathological H&E (hematoxylin & eosin staining, $\times 100$) image shows a moderately-differentiated adenocarcinoma invading the whole layer of rectal wall.

and intraobserver variability confirmed relatively better reproducibility and stability of whole-lesion histogram analysis in combination with rFOV DWI over fFOV DWI in assessment of rectal cancer.

The statistical significance was found in histogram parameters such as ADCmean, 50th, 75th, 90th, and 95th percentile ADCs in assessment of histopathological T staging for both DWI techniques in our study. It was mainly presided by higher percentile ADC in relation to T staging. Some previous studies had similar results, which were consistent with our finding. For instance, both Takahashi *et al.* and Kang *et al.* reported that high percentile ADCs were significantly effective in the differential diagnosis of uterine neoplasm and grading of gliomas^{34,35}. On the other side, Zhang *et al.* and Donati *et al.* reported that the low percentile (5th, 10th, and 25th) ADCs exhibited better diagnostic performances in grading of gastric cancer and prostate cancer aggressiveness^{31,36}. Above investigations demonstrated histogram parameters were useful for histopathological characterization of tumor grading and invasiveness. The low or high percentile ADCs played different roles in assessment of tumor biological features from diverse organs. As for rectal cancer, high percentiles ADCs were found to be significantly meaningful in evaluation of T staging. The low percentile ADCs represented areas with higher cellularity and less water restriction; however, the high percentile ADCs indicated areas with necrotic/cystic components, and less water molecules^{37,38}. One probable explanation for the findings in our study was that rectal cancers with pT3-4 stage often contain many invisible small areas of necrosis and tiny cystic changes, although the conspicuous necrotic and cystic regions were excluded for histogram analysis. The cystic and necrotic components may result in the high frequency of high ADC voxels in contrast to pT1-2 stage tumors, rendering the differentiation between two stages possible.

Moreover, 25th percentile ADC and ADCmin from rFOV DWI were also significantly correlated with histological T staging of rectal cancer. The 25th percentile ADC might indicate the superiority of rFOV DWI over fFOV DWI in detecting regions for tumors with focal areas of high cellularity, which were represented by low percentile ADC³¹. As for the parameter of ADCmin from rFOV DWI, it was correlated positively with T staging. Liu *et al.* found that there was no significant correlation between minimum ADC and T staging of rectal cancer by texture analysis⁵, which was consistent with our finding from fFOV DWI. The proved correlation of ADCmin from rFOV DWI with T stage might be explained by the technical advantage of rFOV DWI over fFOV DWI. The rFOV DWI technique provided images with less distortions and ghosts, rendering anatomic structures of lesions more conspicuous. However, in contrast to our finding from rFOV DWI, Kang *et al.* reported minimum

Parameter/ DWI technique	Cutoff	Sensitivity (%)	Specificity (%)	Area under the curve (AUC)	P-value
ADCmean					
rFOV DWI	1129.06	81.00	85.70	0.850 (0.728, 0.973)	<0.001
fFOV DWI	1057.87	85.70	46.40	0.680 (0.527, 0.834)	0.032
ADCmin					
rFOV DWI	287.50	67.90	81.00	0.714 (0.565, 0.863)	0.011
fFOV DWI	562.50	52.40	50.00	0.590 (0.427, 0.753)	0.284
25th percentile ADC					
rFOV DWI	892.50	81.00	64.30	0.747 (0.598, 0.897)	0.003
fFOV DWI	945.00	52.40	71.40	0.630 (0.468, 0.792)	0.122
50th percentile ADC					
rFOV DWI	1090.00	81.00	85.70	0.839 (0.708, 0.970)	<0.001
fFOV DWI	1057.50	71.40	64.30	0.707 (0.558, 0.857)	0.014
75th percentile ADC					
rFOV DWI	1310.00	76.20	96.40	0.923 (0.849, 0.998)	<0.001
fFOV DWI	1310.00	52.40	89.30	0.762 (0.628, 0.896)	0.002
90th percentile ADC					
rFOV DWI	1527.50	81.00	92.90	0.932 (0.860, 1.000)	<0.001
fFOV DWI	1502.50	61.90	82.10	0.747 (0.609, 0.886)	0.003
95th percentile ADC					
rFOV DWI	1691.00	76.20	89.30	0.878 (0.781, 0.974)	<0.001
fFOV DWI	1460.88	95.20	39.30	0.711 (0.567, 0.855)	0.012
Skewness					
rFOV DWI	0.932	75.00	76.20	0.827 (0.713, 0.940)	<0.001
fFOV DWI	0.760	89.30	57.10	0.747 (0.604, 0.889)	0.003
Kurtosis					
rFOV DWI	1.740	78.60	85.70	0.898 (0.812, 0.984)	<0.001
fFOV DWI	0.984	96.40	52.40	0.791 (0.663, 0.919)	0.001

Table 3. Comparison of ROC analysis of whole-lesion histogram parameters for T1-2 vs. T3-4 stage tumors based on rFOV DWI and fFOV DWI techniques. Note. — Data in parentheses are 95% confidence intervals. ADC values are given in units of 10^{-6} mm²/s.

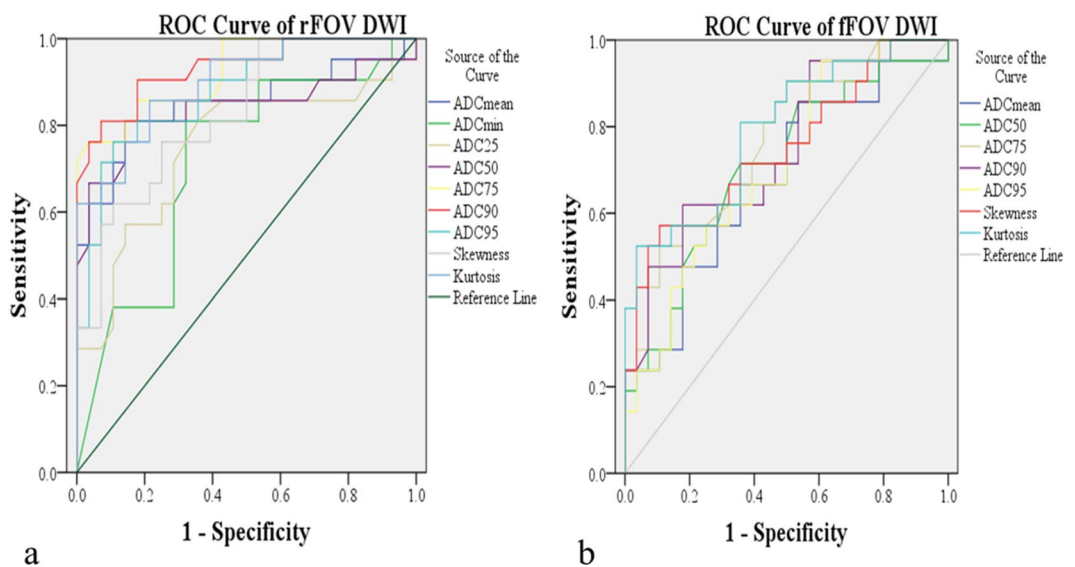


Figure 3. Receiver operating characteristic (ROC) curves demonstrating the false positive rate (sensitivity) and true positive rate (specificity) of whole-lesion histogram parameters for distinguishing pT1-2 and pT3-4 stages of rectal cancer based on rFOV DWI and fFOV DWI techniques. The areas under the ROC curve (AUC) of rFOV DWI (a) for ADCmean, ADCmin, the 25th, 50th, 75th, 90th, and 95th percentiles of ADC values, skewness and kurtosis were 0.850, 0.714, 0.747, 0.839, 0.923, 0.932, 0.878, 0.827 and 0.898 respectively. The areas under the ROC curve (AUC) of fFOV DWI (b) for ADCmean, 50th, 75th, 90th, and 95th percentiles of ADC values, skewness and kurtosis were 0.680, 0.707, 0.762, 0.747, 0.711, 0.747, and 0.791 respectively.

ADC correlated inversely with grading of gliomas³⁵. The different finding of ADC_{min} may be due to the internal features of tumor itself and DWI technique applied. Further investigation is needed to find the actual relationship between ADC_{min} and histological T staging of rectal cancer.

We considered pT1-2 stage rectal cancer was associated with lower skewness and kurtosis, in contrast to pT3-4 stage for both DWI techniques. Theoretically, skewness represents the asymmetry of distribution of ADC values, while kurtosis reflects the peakedness of ADC distribution³³. Higher values of skewness and kurtosis are often associated with more complexities of different components in a given ROI and increased heterogeneity of lesion tissues⁵. The higher-stage rectal tumor was often characterized by more heterogeneous tissue condition and cellular components. This may explain why there were significantly higher kurtosis and skewness in pT3-4 stage than that in pT1-2 stage. The previous study reported comparatively lower value of correlation coefficients for kurtosis (−0.126) and skewness (0.277) in a texture analysis of rectal cancer⁵. The higher results in our study can be explained by the ROI selection method. In our study, the acquisition of histogram parameters was based on whole-lesion covering the whole tumor volume, while the previous texture study was based on single-slice method. The whole-volume method can be more reliable than single-slice method, because it excludes the possibility of variations in selection of single slice^{11,39}.

As for the parameter of entropy, it did not differ significantly between stages of rectal cancer. Entropy refers to statistical measurement of irregularity of gray-level signal intensity (SI) within the volume of interest. Theoretically, higher value of entropy indicates more random distribution of SI and heterogeneity⁴⁰. The negative finding in our study may be caused by relatively small number of patients for each stage of rectal cancer. More patients are needed to verify the significance of entropy in relation to T staging.

In addition, our research found the spearman correlation coefficients demonstrated that the histogram parameters (ADC_{mean}, 50th, 75th, 90th, and 95th percentile ADCs) from both DWI techniques correlated inversely with histological T staging. The histogram metrics from rFOV DWI presented with higher correlation coefficients, which demonstrated superiority of rFOV DWI over fFOV DWI by comparison of above parameters individually. The variability of correlation difference may be mainly caused by utility of different DWI techniques. The rFOV DWI has been reported to provide comparatively good quality and high-resolution images of small structures of rectal lesions over fFOV DWI. The rFOV DWI technique can enlarge the bandwidth along the phase-encoding direction and shorten the readout time, therefore improving the DWI image quality with fewer distortions and susceptibility artifacts.

Limitations. Our study had limitations. First, this was a retrospective study with inevitable biases for patient selection. Second, the sample size was comparatively small, especially for the pT1 stage of rectal cancer. The final result might not reflect the real status of pT1-2 stage. Third, only b values of 0 and 800 s/mm² were applied for analysis. The finding of optimal maximum b value and utility of intravoxel incoherent motion are needed to improve the results of ADC quantification. Fourth, the stratification of patients into T1-T2 or T3-T4 group was not entirely prognostic relevant and not relevant from recent treatment guidelines, which should be mentioned in our study. Finally, according to the latest ESMO (European Society for Medical Oncology) guidelines, patients with cT3a/bN0M0 tumors located in the middle or upper third of the rectum and cT3a/bN1M0 tumors located in the upper third of the rectum could be recommended for major TME surgery without preoperative RT (radiotherapy) or CRT (chemoradiotherapy) treatment. Moreover, as for some patients with cT4aN0M0 tumors located in the upper third of the rectum, ESMO guidelines do not explicitly indicate mandatory preoperative chemoradiation treatment. Besides, some patients with advanced rectal cancer underwent operations because they had complications such as intestinal obstruction or bleeding. Above were the reasons for the enrolled patients with T3 or higher stage of rectal cancer in our hospital having surgical operations without preoperational neoadjuvant treatment.

Conclusion

Our study suggests that whole-lesion histogram analyses of both rFOV DWI and fFOV DWI techniques could help assess rectal cancer invasiveness. The rFOV DWI technique performs better than fFOV DWI technique in assessment of rectal cancer invasiveness.

Materials and Methods

Study population. The Institutional Ethics Review Board approval of Tongji hospital was obtained and informed written consent was waived for this retrospective study. All patient information was treated with confidentiality and used only for the purpose of this study. 112 rectal cancer patients were recruited in this study from April 2016 to February 2017. The inclusion criteria were as follows: 1) patients were enrolled in this study consecutively; 2) patients received no previous neoadjuvant treatment with radiotherapy; 3) patients with pathological confirmation of rectal adenocarcinoma after endoscopy-guided biopsy or surgery (the mucinous adenocarcinoma was not included); 4) patients received both fFOV DWI and rFOV DWI imaging. The exclusion criteria were as follows: 1) patients underwent previous chemoradiotherapy treatment before MR or surgery (n = 25); 2) patients could not fulfill MR scanning (n = 13); 3) patients did not receive surgery after MR (n = 15); 4) poor image quality due to obvious motion artifacts or patient movement (n = 10). The final study cohort was comprised of 49 patients (34 males, 15 females; mean age, 56.2 ± 12.2 years; range, 22–82 years).

MRI examination. All MR examinations were performed by utility of a 3 T scanner (Discovery 750, GE Healthcare, USA) with a 32-channel torso coil. No bowel preparation was given and the intravenous antispasmodic agents were not administered before MR examination. The regular imaging protocol for rectal cancer was as follows: axial T1 FSE (fast spin echo) sequence (TR (repetition time)/TE (echo time), 500/11 msec; section thickness, 5 mm; gap, 1 mm; matrix, 320 × 224; FOV, 380 × 380 mm²); axial T2 FSE sequence (TR/TE, 4050/85

msec; section thickness, 5 mm; gap, 1 mm; matrix, 320×224 ; FOV, 380×380 mm²); and sagittal T2 FSE sequence (TR/TE, 5310/113 msec; section thickness, 3 mm; gap, 0 mm; matrix, 320×320 ; FOV, 250×250 mm²). The scanning of axial imaging was vertical to the long axis of rectal tumor, identified by sagittal T2 sequence.

Two axial DWI sequences including rFOV DWI and fFOV DWI were performed for all patients. The rFOV DWI scanning parameters were as follows: TR/TE, 4000/75 msec; section thickness, 3 mm; gap, 0 mm; matrix, 128×64 ; FOV, 200×100 mm². The fFOV DWI scanning parameters were as follows: TR/TE, 4000/75 msec; section thickness, 3 mm; gap, 0 mm; matrix, 160×128 ; FOV, 400×400 mm². Two b values (0 and 800 s/mm²) were applied in 3 orthogonal directions. The scan time for both DWI techniques was 2 minutes 32 seconds.

Quantitative histogram analysis. All the image data referring to rectal cancer were transferred to the PC and analyzed by utility of in-house developed software (Firevoxel, <https://files.nyu.edu/hr18/public/projects.html>). Two radiologists (with 6 years and 30 years of experience in interpreting abdominal MRI respectively) reviewed all the MR images. The examiners were unaware of histopathological information of patients. Rectal cancers were presented as intraluminal mass or irregular thickening of rectal wall. Rectal lesions were characterized by intermediate high signal on T2WI and high signal on DWI. The examiners performed ROI delineation directly along the border of entire tumor on each slice of DWI images ($b = 800$ s/mm²). T2WI sequence was utilized as reference standard to ensure accurate positioning of ROI. Besides, care was taken to eschew regions of necrotic/cystic components and vessels related to corresponding slice. In addition, the lowest and highest slices of DWI images were excluded for partial volume effects. After all the ROIs were determined on the DWI images, the histogram parameters were automatically calculated by using Firevoxel software and SPSS v. 19.0 (IBM, Armonk, NY, USA). The histogram parameters were comprised of ADC_{mean} (mean ADC value), ADC_{max} (maximum ADC value), ADC_{min} (minimum ADC value), 5th, 10th, 25th, 50th (or median), 75th, 90th and 95th percentiles, skewness, kurtosis, entropy and tumor volume.

Surgery and pathological evaluation. All the eligible patients underwent curative surgery or palliative operations. The median time interval between surgery and MRI scan was 4 days (range, 1–6 days). The surgical specimens were stained with hematoxylin and eosin for histopathological evaluation. The microscopic histological analysis of resected specimens was performed by a pathologist with 25 years' experience, who was also blinded to clinical and histopathological information of patients. The histological type and T staging were assessed and recorded according to the 7th edition of TNM system for rectal cancer by the American Joint Committee on Cancer (AJCC).

Statistical analysis. The interobserver and intraobserver agreements were interpreted utilizing the intra-class correlation coefficient (ICC) test (0.00–0.20, poor; 0.21–0.40, fair; 0.41–0.60, moderate; 0.61–0.80, good; and 0.81–1.00, excellent). The histogram parameters were compared between pT1-2 and pT3-4 stages by independent student t test or the Man-Whitney U-test with Bonferroni correction according to the results of normal distribution test. The Spearman correlation analysis test was performed to evaluate the relationship between histogram parameters and T staging of rectal cancer for both rFOV DWI and fFOV DWI (0.00–0.19, very weak; 0.20–0.39, weak; 0.40–0.59, moderate; 0.60–0.79, strong; 0.80–1.00, very strong). Receiver operating characteristic (ROC) curve analysis was performed to determine the diagnostic performance of histogram parameters in distinguishing T staging of rectal cancer based on two DWI techniques. We also examined the area under the ROC curve (AUC) to evaluate the diagnostic abilities of ADC values, skewness and kurtosis from rFOV DWI and fFOV DWI. The AUC values of different histogram parameters from both DWI techniques were compared by Z tests.

All the statistical analyses were performed using SPSS v. 19.0 (IBM, Armonk, NY, USA) and MedCalc software (version 12.7.0.0; Mariakerke, Belgium). Values of $P < 0.05$ were considered significant.

Compliance with ethical standards. This study involving human participants was approved by the Institutional Review Board (IRB) of Tongji hospital, and we pledged to abide by the declaration of Helsinki (2000 EDITION) in accordance with the relevant medical research rules of China in the study. Written informed consent was waived from all patients. All patient-sensitive information was kept with confidentiality and used only for the purpose of the study.

Data availability

The datasets generated and analyzed during the current study are available from the corresponding author on reasonable request.

Received: 28 January 2019; Accepted: 18 November 2019;

Published online: 10 December 2019

References

- Jemal, A., Siegel, R., Xu, J. & Ward, E. Cancer statistics, 2010. *CA. Cancer. J. Clin.* **60**, 277–300 (2010).
- Zhang, G., Cai, Y. Z. & Xu, G. H. Diagnostic Accuracy of MRI for Assessment of T Category and Circumferential Resection Margin Involvement in Patients With Rectal Cancer: A Meta-Analysis. *Dis. Colon. Rectum.* **59**, 789–799 (2016).
- Peeters, K. C. *et al.* The TME trial after a median follow-up of 6 years: increased local control but no survival benefit in irradiated patients with resectable rectal carcinoma. *Ann Surg.* **246**, 693–701 (2007).
- Kim, H. *et al.* Rectal cancer: comparison of accuracy of local-regional staging with two- and three-dimensional preoperative 3-T MR imaging. *Radiology.* **254**, 485–492 (2010).
- Liu, L. *et al.* Application of texture analysis based on apparent diffusion coefficient maps in discriminating different stages of rectal cancer. *J. Magn. Reson. Imaging.* **45**, 1798–1808 (2017).
- Kim, S. H. *et al.* Diagnostic accuracy of 3.0-Tesla rectal magnetic resonance imaging in preoperative local staging of primary rectal cancer. *Invest. Radiol.* **43**, 587–593 (2008).
- Sauer, R. *et al.* Preoperative versus postoperative chemoradiotherapy for rectal cancer. *N. Engl. J. Med.* **351**, 1731–1740 (2004).

8. Al-Sukhni, E. *et al.* Diagnostic accuracy of MRI for assessment of T category, lymph node metastases, and circumferential resection margin involvement in patients with rectal cancer: a systematic review and meta-analysis. *Ann. Surg. Oncol.* **19**, 2212–2223 (2012).
9. van der Pol, C. B., Shabana, W. M., McInnes, M. D. & Schieda, N. High-resolution T2-weighted (T2W) oblique plane turbo spin-echo (TSE) MRI for rectal adenocarcinoma staging. *Clin. Imaging.* **39**, 627–631 (2015).
10. Attenberger, U. I. *et al.* Multi-parametric MRI of rectal cancer - do quantitative functional MR measurements correlate with radiologic and pathologic tumor stages? *Eur. J. Radiol.* **83**, 1036–1043 (2014).
11. Lambregts, D. M. *et al.* Tumour ADC measurements in rectal cancer: effect of ROI methods on ADC values and interobserver variability. *Eur. Radiol.* **21**, 2567–2574 (2011).
12. Attenberger, U. I. *et al.* Quantitative Perfusion Analysis of the Rectum Using Golden-Angle Radial Sparse Parallel Magnetic Resonance Imaging: Initial Experience and Comparison to Time-Resolved Angiography With Interleaved Stochastic Trajectories. *Invest. Radiol.* **52**, 715–724 (2017).
13. Gollub, M. J. *et al.* Does gadolinium-based contrast material improve diagnostic accuracy of local invasion in rectal cancer MRI? A multireader study. *Am. J. Roentgenol.* **204**, W160–W167 (2015).
14. Nougaret, S. *et al.* The use of MR imaging in treatment planning for patients with rectal carcinoma: have you checked the “DISTANCE”? *Radiology.* **268**, 330–344 (2013).
15. Kobayashi, S. *et al.* Diagnostic performance of diffusion-weighted magnetic resonance imaging in bladder cancer: potential utility of apparent diffusion coefficient values as a biomarker to predict clinical aggressiveness. *Eur. Radiol.* **21**, 2178–2186 (2011).
16. Lambregts, D. M. J. *et al.* Diffusion-weighted MRI to assess response to chemoradiotherapy in rectal cancer: main interpretation pitfalls and their use for teaching. *Eur. Radiol.* **27**, 4445–4454 (2017).
17. Curvo-Semedo, L. *et al.* Diffusion-weighted MRI in rectal cancer: apparent diffusion coefficient as a potential noninvasive marker of tumor aggressiveness. *J. Magn. Reson. Imaging.* **5**, 1365–1371 (2012).
18. Lu, Z. H., Hu, C. H., Qian, W. X. & Cao, W. H. Preoperative diffusion-weighted imaging value of rectal cancer: preoperative T staging and correlations with histological T stage. *Clin. Imaging.* **40**, 563–568 (2016).
19. Sun, Y. *et al.* Apparent Diffusion Coefficient (ADC) value: a potential imaging biomarker that reflects the biological features of rectal cancer. *PLoS one.* **9**(10), e109371 (2014).
20. Hao, Y. *et al.* Differentiation between malignant and benign thyroid nodules and stratification of papillary thyroid cancer with aggressive histological features: whole-lesion diffusion-weighted imaging histogram analysis. *J. Magn. Reson. Imaging.* **44**, 1546–1555 (2016).
21. Li, A. *et al.* Subtype Differentiation of Small (≤ 4 cm) Solid Renal Mass Using Volumetric Histogram Analysis of DWI at 3-T MRI. *Am. J. Roentgenol.* **211**, W1–W10 (2018).
22. Park, J. Y. *et al.* Comparison of readout segmented echo planar imaging (EPI) and EPI with reduced field-of-view diffusion-weighted imaging at 3t in patients with breast cancer. *J. Magn. Reson. Imaging.* **42**, 1679–1688 (2015).
23. Zaharchuk, G. *et al.* Reduced field-of-view diffusion imaging of the human spinal cord: comparison with conventional single-shot echo-planar imaging. *Am. J. Neuroradiol.* **32**, 813–820 (2011).
24. Bhosale, P. *et al.* Feasibility of a reduced field-of-view diffusion-weighted (rFOV) sequence in assessment of myometrial invasion in patients with clinical FIGO stage I endometrial cancer. *J. Magn. Reson. Imaging.* **43**, 316–324 (2016).
25. Peng, Y. *et al.* Comparison of reduced field-of-view diffusion-weighted imaging (DWI) and conventional DWI techniques in the assessment of rectal carcinoma at 3.0T: Image quality and histological T staging. *J. Magn. Reson. Imaging.* **47**, 967–975 (2018).
26. Nguyen, H. T. *et al.* Non-invasive quantification of tumour heterogeneity in water diffusivity to differentiate malignant from benign tissues of urinary bladder: a phase I study. *Eur. Radiol.* **27**, 2146–2152 (2017).
27. Tozer, D. J. *et al.* Apparent diffusion coefficient histograms may predict low-grade glioma subtype. *NMR. Biomed.* **20**, 49–57 (2007).
28. Davnall, F. *et al.* Assessment of tumor heterogeneity: an emerging imaging tool for clinical practice? *Insights. Imaging.* **3**, 573–589 (2012).
29. Just, N. Improving tumour heterogeneity MRI assessment with histograms. *Br. J. Cancer.* **111**, 2205–2213 (2014).
30. De Cecco, C. N. *et al.* Texture analysis as imaging biomarker of tumoral response to neoadjuvant chemoradiotherapy in rectal cancer patients studied with 3-T magnetic resonance. *Invest. Radiol.* **50**, 239–245 (2015).
31. Donati, O. F. *et al.* Prostate cancer aggressiveness: assessment with whole-lesion histogram analysis of the apparent diffusion coefficient. *Radiology.* **271**, 143–152 (2014).
32. Rosenkrantz, A. B. *et al.* Whole-lesion diffusion metrics for assessment of bladder cancer aggressiveness. *Abdom. Imaging.* **40**, 327–332 (2015).
33. Umanodan, T. *et al.* ADC histogram analysis for adrenal tumor histogram analysis of apparent diffusion coefficient in differentiating adrenal adenoma from pheochromocytoma. *J. Magn. Reson. Imaging.* **45**, 1195–1203 (2017).
34. Takahashi, M. *et al.* Utility of histogram analysis of apparent diffusion coefficient maps obtained using 3.0T MRI for distinguishing uterine carcinosarcoma from endometrial carcinoma. *J. Magn. Reson. Imaging.* **43**, 1301–1307 (2016).
35. Kang, Y. *et al.* Gliomas: Histogram analysis of apparent diffusion coefficient maps with standard- or high-b-value diffusion-weighted MR imaging—correlation with tumor grade. *Radiology.* **261**, 882–890 (2011).
36. Zhang, Y. *et al.* Assessment of histological differentiation in gastric cancers using whole-volume histogram analysis of apparent diffusion coefficient maps. *J. Magn. Reson. Imaging.* **45**, 440–449 (2017).
37. Xue, H. *et al.* Histogram analysis of apparent diffusion coefficient for the assessment of local aggressiveness of cervical cancer. *Arch. Gynecol. Obstet.* **290**, 341–348 (2014).
38. Shindo, T. *et al.* Histogram Analysis of Apparent Diffusion Coefficient in Differentiating Pancreatic Adenocarcinoma and Neuroendocrine Tumor. *Medicine.* **95**, e2574 (2016).
39. Choi, M. H. *et al.* Diffusion-weighted imaging: Apparent diffusion coefficient histogram analysis for detecting pathologic complete response to chemoradiotherapy in locally advanced rectal cancer. *J. Magn. Reson. Imaging.* **44**, 212–220 (2016).
40. Liu, S. *et al.* Whole-volume apparent diffusion coefficient-based entropy parameters for assessment of gastric cancer aggressiveness. *J. Magn. Reson. Imaging.* **47**, 168–175 (2018).

Author contributions

Zhen Li conceived the experiment; Daoyu Hu designed the experiment; Xuemei Hu performed the experiment; Hao Tang analyzed the data; Yaqi Shen performed the statistical analysis; Ihab Kamel contributed to manuscript editing and reviewing; Yang Peng wrote the original draft.

Competing interests

The authors declare no competing interests.

Additional information

Correspondence and requests for materials should be addressed to Z.L.

Reprints and permissions information is available at www.nature.com/reprints.

Publisher's note Springer Nature remains neutral with regard to jurisdictional claims in published maps and institutional affiliations.



Open Access This article is licensed under a Creative Commons Attribution 4.0 International License, which permits use, sharing, adaptation, distribution and reproduction in any medium or format, as long as you give appropriate credit to the original author(s) and the source, provide a link to the Creative Commons license, and indicate if changes were made. The images or other third party material in this article are included in the article's Creative Commons license, unless indicated otherwise in a credit line to the material. If material is not included in the article's Creative Commons license and your intended use is not permitted by statutory regulation or exceeds the permitted use, you will need to obtain permission directly from the copyright holder. To view a copy of this license, visit <http://creativecommons.org/licenses/by/4.0/>.

© The Author(s) 2019